Matrix Polyelectrolyte Microcapsules: New System for Macromolecule Encapsulation

ARTICLE *in* LANGMUIR · MAY 2004

Impact Factor: 4.46 · DOI: 10.1021/la036177z · Source: PubMed

4 AUTHORS, INCLUDING:

Dmitry Volodkin
Fraunhofer Institute for Biomedical Engineer…
77 PUBLICATIONS **2,712** CITATIONS
SEE PROFILE

Gleb Sukhorukov
Queen Mary, University of London
318 PUBLICATIONS **19,395** CITATIONS
SEE PROFILE

Matrix Polyelectrolyte Microcapsules: New System for Macromolecule Encapsulation

Dmitry V. Volodkin,[†,‡] Alexander I. Petrov,[§] Michelle Prevot,[†] and Gleb B. Sukhorukov*[,†]

Max-Planck Institute of Colloids and Interfaces, Golm/Potsdam, 14476, Germany, Department of Chemistry, Moscow State University, Moscow, 119992, Russia, and Institute of Theoretical and Experimental Biophysics, Pushchino, Moscow Region, 142290, Russia

Received November 19, 2003. In Final Form: January 26, 2004

A new approach to fabricate polyelectrolyte microcapsules is based on exploiting porous inorganic microparticles of calcium carbonate. Porous $CaCO_3$ microparticles (4.5−5.0 microns) were synthesized and characterized by scanning electron microscopy and the Brunauer−Emmett−Teller method of nitrogen adsorption/desorption to get a surface area of 8.8 m^2/g and an average pore size of 35 nm. These particles were used as templates for polyelectrolyte layer-by-layer assembly of two oppositely charged polyelectrolytes, poly(styrene sulfonate) and poly(allylamine hydrochloride). Calcium carbonate core dissolution resulted in formation of polyelectrolyte microcapsules with an internal matrix consisting of a polyelectrolyte complex. Microcapsules with an internal matrix were analyzed by confocal Raman spectroscopy, scanning electron microscopy, force microscopy, and confocal laser-scanning fluorescence microscopy. The structure was found to be dependent on a number of polyelectrolyte adsorption treatments. Capsules have a very high loading capacity for macromolecules, which can be incorporated into the capsules by capturing them from the surrounding medium into the capsules. In this paper, we investigated the loading by dextran and bovine serum albumin as macromolecules. The amount of entrapped macromolecules was determined by two independent methods and found to be up to 15 pg per microcapsule.

Introduction

Encapsulation of various substances into different micro- and nanoparticles such as capsules, polymer spheres, liposomes, and so forth has received considerable attention due to increased interest in biotechnology, medicine, catalysis, ecology, nutrition, and so forth. Sequential layer-by-layer (LbL) polyelectrolyte adsorption was used to fabricate multilayer films onto flat macroscopic substrates utilizing electrostatic interaction between oppositely charged macromolecules at each adsorption step.[1] The extension of this technology toward colloidal species has enabled an alternating polyelectrolyte assembly on different kinds of supports.[2] Encapsulation of macromolecules, proteins, and other bioactive materials into such type of microcapsules is of great interest for pharmaceutics and biotechnology due to the possibilities to apply such systems as micro- and nanocontainers for drug delivery and controlled release and in catalysis.

At present, there are two general approaches to how to encapsulate the biomacromolecules into polyelectrolyte capsules using the LbL technique. The first method consists of formation of particles out of molecules subjected to encapsulation. Dye and drug nanocrystals,[3] protein aggregates, and compact forms of DNA[4] were used to template LbL assembly thus leading to encapsulation. The second approach for encapsulation of macromolecules exploits preformed hollow capsules and incorporates the macromolecules from the surrounding medium by switching the permeability of the hollow capsule shell.[5] Recently, incorporation of charged and noncharged macromolecules has been achieved via fabrication of double-walled capsules with subsequent decomposition of the inner wall.[6] Moreover, polymer encapsulation via controlled polymeric synthesis inside the capsule has also been demonstrated.[7] These approaches have some disadvantages such as formation of stable cores with certain surface properties for the first method, low incorporation efficiency for the second one, and confined usage of employed polymers for the other approaches. Another obstacle of considerable importance, which hinders the functional encapsulation of the biomacromolecules, is the harsh conditions usually used for core decomposition (extreme pH or usage of organic solvents and oxidizing agents).

* Corresponding author. Tel: +49-331-567-9429. Fax: +49-331-567-9202. E-mail: gleb@mpikg-golm.mpg.de.

† Max-Planck Institute of Colloids and Interfaces.

‡ Moscow State University.

§ Institute of Theoretical and Experimental Biophysics.

(1) (a) Decher, G.; Hong, J. D. *Macromol. Chem., Macromol. Symp.* **1991**, *46*, 321. (b) Decher, G.; Hong, J. D.; Schmitt, J. *Thin Solid Films* **1992**, *210* (1−2), 831.

(2) (a) Bertrand, P.; Jonas, A.; Laschewsky, A.; Legras, R. *Macromol. Rapid Commun.* **2000**, *21*, 319. (b) Sukhorukov, G. B. In *Studies in Interface Science*; Möbius, D., Miller, R., Eds.; Elsevier: Amsterdam, 2001; p 383.

(3) (a) Qiu, X.; Leporatti, S.; Donath, E.; Möhwald, H. *Langmuir* **2001**, *17*, 5375. (b) Antipov, A. A.; Sukhorukov, G. B.; Donath, E.; Möhwald, H. *J. Phys. Chem. B* **2001**, *105* (12), 2281. (c) Ai, H.; Jones, S.; Villiers, M. M.; Lvov, Y. M. *J. Controlled Release* **2003**, *86*, 59.

(4) (a) Bobreshova, M. E.; Sukhorukov, G. B.; Saburova, E. A.; Elfimova, L. I.; Sukhorukov, B. I.; Shabarchina, L. I. *Biophysics* **1999**, *44*, 813. (b) Trubetskoy, V. S.; Loomis, A.; Hagstrom, J. E.; Budker, V. G.; Wolff, J. A. *Nucleic Acids Res.* **1999**, *27*, 3090. (c) Volodkin, D. V.; Balabushevitch, N. G.; Sukhorukov, G. B.; Larionova, N. I. *STP Pharm. Sci.* **2003**, *13* (3), 163. (d) Volodkin, D. V.; Balabushevitch, N. G.; Sukhorukov, G. B.; Larionova, N. I. *Biochemistry* (*Moscow*) **2003**, *68* (2), 283.

(5) (a) Donath, E.; Sukhorukov, G. B.; Caruso, F.; Davis, S. A.; Möhwald, H. *Angew. Chem., Int. Ed.* **1998**, *37* (16), 2202. (b) Sukhorukov, G. B.; Antipov, A. A.; Voigt, A.; Donath, E.; Möhwald, H. *Macromol. Rapid Commun.* **2001**, *22* (1), 44. (c) Tiourina, O. P.; Antipov, A. A.; Sukhorukov, G. B.; Larionova, N. I.; Lvov, Y.; Möhwald, H. *Macromol. Biosci.* **2001**, *1*, 209. (d) Lvov, Y.; Antipov, A. A.; Mamedov, A.; Möhwald, H.; Sukhorukov, G. B. *Nano Lett.* **2001**, *1* (3), 125.

(6) (a) Radchenko, I. L.; Sukhorukov, G. B.; Möhwald, H. *Colloids Surf., A* **2000**, *202*, 127. (b) Radchenko, I. L.; Sukhorukov, G. B.; Leporatti, S.; Khomutov, G. B.; Donath, E.; Möhwald, H. *J. Colloid Interface Sci.* **2000**, *230*, 272.

(7) Dähne, L.; Leporatti, S.; Donath, E.; Möhwald, H. *J. Am. Chem. Soc.* **2001**, *123*, 5431.

10.1021/la036177z CCC: $27.50
Published on Web 03/09/2004

This work aims to elaborate a new approach for fabrication of polyelectrolyte capsules employing porous inorganic $CaCO_3$ microparticles as a template for polyelectrolyte capsule fabrication. Microcapsule formation is based on consecutive core coatings in solutions of two oppositely charged polyelectrolytes (poly(styrene sulfonate) and poly(allylamine hydrochloride)) followed by core dissolution. The structures formed were studied by scanning electron and force microscopy and confocal Raman and laser-scanning fluorescence microscopy. The structure and properties of particles used in this study and the capacity of microcapsules for macromolecule entrapment will be discussed as well.

Materials and Methods

The sources of the chemicals are as follows: sodium poly(styrene sulfonate) (PSS, $M_w \approx 70$ kDa) and poly(allylamine hydrochloride) (PAH, $M_w \approx 70$ kDa) (Aldrich, USA), fluorescein isothiocyanate (FITC, Sigma, USA), ethylenediaminetetraacetic acid (EDTA, Sigma), calcium chloride dihydrate ($CaCl_2 \cdot 2H_2O$, Ultra, Sigma), Na_2CO_3 (pro analysis, Merck, Germany), bovine serum albumin (BSA, Sigma), and dextran−FITC (4 kDa, Aldrich). All materials were used without further purification. The water used in all experiments was prepared in a three-stage Millipore Milli-Q Plus 185 purification system and had a resistivity higher than 18.2 MΩ cm.

Fabrication of $CaCO_3$ Microparticles. Uniform, nearly spherical microparticles of $CaCO_3$ with a narrow size distribution were prepared by colloidal crystallization from supersaturated (relative to $CaCO_3$) solution. The process was initiated by rapid mixing of equal volumes of $CaCl_2$ and Na_2CO_3 solutions. The mixture was intensively agitated on a magnetic stirrer. The time course of the reaction was observed under a light microscope. The amorphous precipitate instantly formed upon mixing was found to transform more slowly into microparticles with spherical morphology. The diameter of microparticles increases with time up to 15−20 μm without an essential change in particle morphology.

In parallel with colloidal aggregation of primary nanoparticles of $CaCO_3$ into microspheres, the true crystallization of $CaCO_3$ into rhombohedral calcite microcrystals is also observed. We have found experimental conditions for $CaCO_3$ crystallization practically excluding the formation of all $CaCO_3$ microparticles except for microspherical ones.

In a typical experiment, 0.33 M Na_2CO_3 solution (sodium carbonate was found to give more reproducible results in comparison with ammonium bicarbonate used in ref 8) was rapidly poured into an equal volume of 0.33 M solution of $CaCl_2$ at room temperature, and after intense agitation on a magnetic stirrer the precipitate was filtered off, thoroughly washed with pure water, and dried in air. The procedure results in highly homogeneous, spherical $CaCO_3$ microparticles with an average diameter ranging from 4 to 6 μm.

Microcapsule Preparation. Polyelectrolyte microcapsules were prepared by alternating incubation of $CaCO_3$ microparticles (1% w/w in suspension) in PSS and PAH solutions (2 mg mL^{-1}), within 0.5 M NaCl. The pH of the polymer solutions was adjusted to 6.5 by addition of HCl/NaOH. Each adsorption cycle (10 min incubation, shaking) was completed with three centrifugation steps (200*g*, 5 min) followed by suspension in water containing 0.05 M NaCl for 4 min. Washing procedures were used before the next polyelectrolyte was added and were applied to remove nonbound polymer. Thus, a desirable number of polyelectrolyte adsorption procedures (PEAP) was achieved. The last washing step was carried out in pure water. Then the treated microparticles were resuspended in an Eppendorf tube by adding 0.1 M EDTA solution (pH 7.0 was adjusted by HCl) to dissolve the calcium carbonate core. After 30 min of agitation, the capsules were centrifuged (1500*g*, 5 min), the supernatant was removed, and the capsules were resuspended in fresh EDTA. This washing procedure with EDTA was repeated three times; the resultant suspension of the formed microcapsules was washed four times with pure water and stored at 4 °C in water. The concentration of $CaCO_3$ particles and formed capsules was calculated with a bright-line hematocytometer (cell counting chamber, Sigma).

To fabricate microcapsules with fluorescent-labeled polyelectrolyte, the same procedure was used with PAH−FITC. To prepare PAH−FITC, two solutions (PAH and FITC) were mixed in 50 mM borate buffer (pH 9.5) at a ratio of 100:1 (amino group of PAH/FITC) and dialyzed against water overnight after 2 h of incubation at room temperature.

Encapsulation of Macromolecules into Polyelectrolyte Microcapsules. BSA was labeled with FITC by mixing of BSA and FITC solutions in 50 mM borate buffer (pH 9.5) at a molar ratio of 1:1. After stirring for 2 h at room temperature, the solution was dialyzed against water overnight and used for further study. Suspensions of microcapsules (6 and 16 PEAP) in water (100 μL) with the concentration (3−5) × 10^6 capsules/mL were added to 400 μL of BSA−FITC or dextran−FITC water solution (2.5 mg mL^{-1}) and were shaken for 1 h. Then the suspension was washed three times with pure water using the centrifugation protocol (2000*g*, 5 min). The volume of the microcapsule suspension was adjusted to 150 μL with water, and the capsule concentration was calculated as described above. Three microliters of the suspension was used for quartz crystal microbalance analysis, and 100 μL was withdrawn for determination of BSA or dextran content. For this procedure, an equal volume of 0.1 M NaOH was added to the suspension. The resulting 200 μL of this clean solution (microcapsules dissolve at a pH higher than 12) was poured together with 2.8 mL of 0.2 M phosphate buffer solution (PBS, pH 7.4). Then the fluorescence of the solution was measured. The same operation was carried out using BSA−FITC and dextran−FITC solutions with various concentrations from 3 × 10^{-3} to 3 × 10^{-1} mg mL^{-1} instead of the microcapsule suspension. The amount of BSA−FITC and dextran−FITC in microcapsules was found by comparing a signal from samples of capsules and reference solutions of BSA−FITC and dextran−FITC. To check the influence of the microcapsule components, PSS and PAH, on the fluorescence measurements, microcapsules were added to reference solutions of BSA−FITC and dextran−FITC, at the same concentration of capsules as the samples with entrapped BSA−FITC or dextran−FITC. A suspension of capsules before macromolecule entrapment (100 μL, (3−5) × 10^6 capsules/mL) was used to get a background signal.

Scanning Electron Microscopy (SEM). For SEM analysis, samples were prepared by applying a drop of the particle suspension to a glass slide and then drying overnight. Then samples were sputtered with gold and measurements were conducted using a Gemini Leo 1550 instrument at an operation voltage of 3 keV.

Scanning Force Microscopy (SFM). The micrographs were obtained by means of a Digital Instruments Nanoscope IIIa Multimode SFM (Digital Instruments Inc., Santa Barbara, CA) in air at room temperature using tapping mode. A drop of sample suspension was applied to a freshly cleaved mica support.

Confocal Laser-Scanning Fluorescence Microscopy (CLSM). Confocal micrographs were taken with a Leica confocal scanning system mounted to a Leica Aristoplan and equipped with a 100× oil immersion objective with a numerical aperture (NA) of 1.4. The excitation wavelength was 488 nm. In Figure 3, the size distribution is presented with the percentage of particles versus the size. The data were obtained using the optical images.

Fluorescence Microscopy. Fluorescence spectra were recorded using Fluorolog, Spex. (Germany). The excitation wavelength was chosen to be 488 nm according to the FITC-labeled substrates.

Raman Spectroscopy. Raman spectra and images were made in clean water using a Confocal Raman Microscope (CRM200, Witec) with a piezo scanner (P-500, Physik Instrumente) and objectives (60×, NA = 0.80, or 100× oil, NA = 1.25, Nikon). In a typical experiment, a circularly polarized laser (CrystaLaser, $\lambda = 532$ nm) was focused on the sample with diffraction-limited spot size ($\sim\lambda/2$). An avalanche photodiode detector (APD) was used to record high-resolution Raman images. For local Raman spectroscopic analysis of the microparticle, we focused the beam spot either exactly inside the spherical particle or, for measuring onto the surface of particles, it was focused on the edge. For each sample, three different microcapsules were measured.

(8) Antipov, A. A.; Shshukin, D.; Fedutik, Y.; Petrov, A. I.; Sukhorukov, G. B.; Möhwald, H. *Colloids Surf., A* **2003**, *224*, 175.

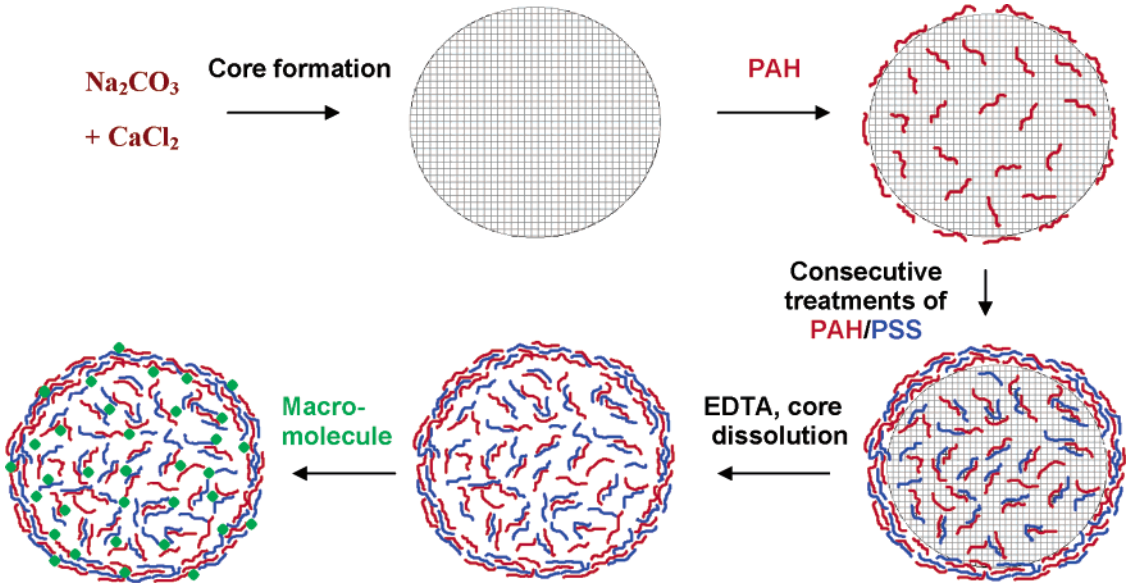

Figure 1. Scheme of capsule fabrication and encapsulation of macromolecules into capsules.

Quartz Crystal Microbalance (QCM). To perform microgravimetric measurements, the quartz crystal microbalance technique (USI-System, Japan) was used. An AT-cut 9 MHz Au/quartz crystal electrode (surface area, 0.16 cm^2; mass sensitivity, 0.87 ng Hz^{-1}) was employed as a working electrode. In the measurements, 3 μL of a suspension of native microcapsules or microcapsules loaded with BSA or dextran in pure water with a certain particle concentration was dropped on the QCM electrode and dried for 20 min in an oven at 65 °C.

Brunauer−Emmett−Teller (BET) Method. The surface area and the pore size distribution of $CaCO_3$ microparticles were determined following the Brunauer−Emmett−Teller method of nitrogen adsorption/desorption at 77 K, the data being collected with a Micromeritics TriStar system.

Energy Dispersive X-ray (EDX) Analysis. EDX analysis was performed on samples prepared similarly to the SEM samples. The analysis was done with a Link EDX system from Oxford Instruments with an optimal resolution of 133 eV.

Electrophoretic Mobility. Electrophoretic mobilities of $CaCO_3$ microparticles were measured in water suspension using a Malvern Zetasizer 4. Small particles were collected from the suspension due to quick sedimentation.

Results and Discussion

Fabrication of Microcapsules. A novel approach to fabricate matrix type polyelectrolyte microcapsules and a technique of macromolecule encapsulation into the capsules were developed. The scheme illustrating this method is depicted in Figure 1. According to the scheme, the porous inorganic $CaCO_3$ microparticles were fabricated by mixing two salt solutions at appropriate conditions. These particles were used as sacrificial templates (microcores) for capsule fabrication using the LbL method with PSS and PAH as the polyelectrolytes. This resulted in the formation of polyelectrolyte complex not only on the surface of the microcores but also within the interior of the porous supports due to diffusion of polyelectrolytes inside. The next step is core dissolution by extraction of calcium by complexation with EDTA leading to the formation of the microcapsule as presented in Figure 1. The complex, formed in the polyelectrolyte matrix upon sequential layer deposition, remains within the microcapsule. This matrix is reinforced by the outer shell made of the same polyelectrolytes on the particle surface.

Fabrication of porous $CaCO_3$ microparticles is a very important point in our study. Crystallization of calcium carbonate from supersaturated solutions has been the subject of many studies due to its great importance in geo-, bio-, and material sciences, as well as due to its wide applications in industry, technology, medicine, and many other fields. Many efforts have been made to elucidate formation of inorganic nanoparticles in saturated solutions,[9c] the kinetics and mechanisms of crystallization, and also mutual transformations between calcium carbonate polymorphs: calcite, aragonite, and vaterite.[9,10] As a rule, the direct mixing of soluble salts of Ca^{2+} and CO_3^{2-} results initially in an amorphous precipitate, which transforms further to aggregated $CaCO_3$ microcrystals with a different morphology.

Great practical needs in preparation of $CaCO_3$ consisting of uniform, homogeneous size, and nonaggregated microparticles stimulated many studies on searching for ways to control the crystallization process. The quality of the resulting microparticles was found to be strongly dependent on the experimental conditions such as the type of salts used, their concentration, pH, temperature and rate of mixing of the solutions, and the intensity of agitation of the reaction mixture probably through their effect on the rate of the nucleation process.[9,10]

Different additives to the reaction mixture such as divalent cations, organic solvents, and both synthetic and natural macromolecules were shown to exert a profound effect on the morphology of the $CaCO_3$ microparticles formed.[11] However, despite great efforts the problem of controllable crystallization of $CaCO_3$ resulting in macroscopic quantities of uniform, homogeneous, and nonaggregated $CaCO_3$ micro- and nanoparticles remains to be solved.

We have developed a simple and reproducible procedure for preparation of spherical $CaCO_3$ microparticles with a rather narrow size distribution ranging for the most part

(9) (a) Tracy, L. S.; François, C. J. P.; Jennings, H. M. *J. Cryst. Growth* **1998**, *193*, 374. (b) Koga, N.; Nakagoe, Y.; Tanaka, H. *Thermochim. Acta* **1998**, *318*, 239. (c) Horn, D.; Rieger, *Angew. Chem., Int. Ed.* **2001**, *40*, 4330.

(10) (a) Ogino, T.; Suzuki, T.; Sawad, K. *Geochim. Cosmochim. Acta* **1987**, *51*, 2757. (b) Spanos, N.; Koutsoukos, P. G. *J. Cryst. Growth* **1998**, *191*, 783. (c) Kitamura, M. *J. Colloid Interface Sci.* **2001**, *236*, 318. (d) Kitamura, M.; Konno, H.; Yasui, A.; Masuoka, H. *J. Cryst. Growth* **2002**, *236*, 323.

(11) (a) Kato, T.; Susuki, T.; Amamiya, T.; Irie, T.; Komiyama, M.; Yui, H. *Supramol. Sci.* **1998**, *5*, 411. (b) Manoli, F.; Dalas, E. *J. Cryst. Growth* **2000**, *218*, 359. (c) Cölfen, H.; Qi, L. *Chem.—Eur. J.* **2001**, *7*, 106.

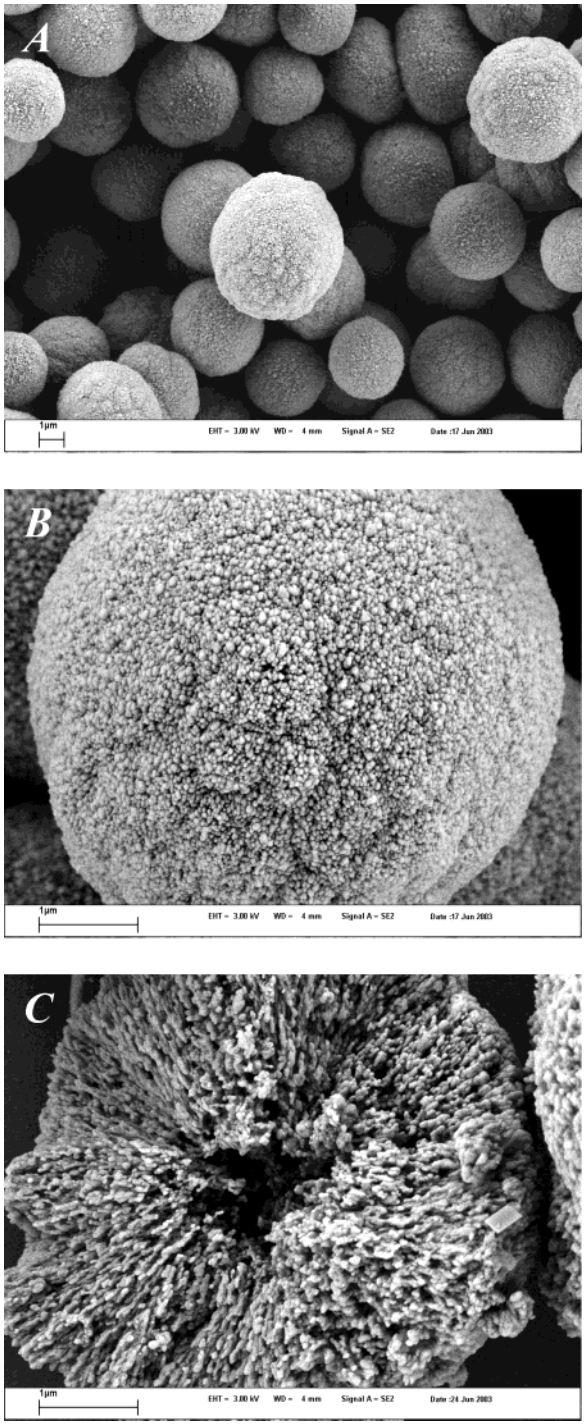

Figure 2. SEM images of $CaCO_3$ microparticles: (A) in overview, (B) single particle, and (C) broken particle. Scale bar = 1 μm.

from 4 to 6 μm that is shown in Figure 3A. SEM images of these microparticles are presented in Figure 2. The shape of the $CaCO_3$ microsupports prepared is nearly spherical as shown in Figure 2A. The surface morphology of the microparticle is presented in Figure 2B. One can see that the surface is very rough and consists of a great number of carbonate nanoparticles combined to form the specific morphology. Figure 2C shows the cross section of a broken microparticle illustrating the internal structure, which has canal-like structure having a pore size in the range of tens of nanometers.

The average weight of one microparticle was determined to be 88 pg by QCM. The volume of the particle is $V = 4/3\pi r^3 = 5.6 \times 10^{-17}$ m^3, where r is the average radius ($r = d/2 = 2.4 \times 10^{-6}$ m, d is the average diameter, Figure 3A). The average density of one porous $CaCO_3$ microparticle is $\rho = m/V = 1.6$ g/cm^3. The density of calcium carbonate is 2.7 g/cm^3. In such a way of estimation, about 59% of the particle volume is occupied with solid $CaCO_3$ and about 41% is the volume of internal pores.

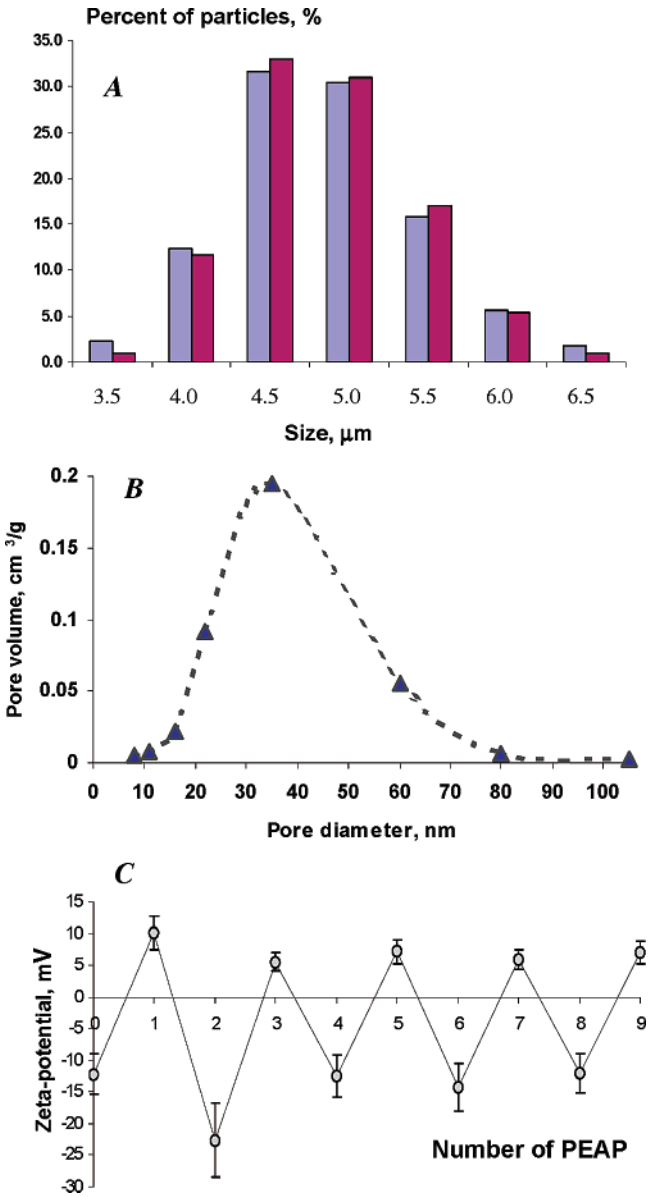

Figure 3. (A) Size distribution of $CaCO_3$ microparticles (brown) and microcapsules prepared on these particles (blue); 6 PEAP. (B) Pore size distribution of $CaCO_3$ microparticles. (C) ξ-Potential as a function of PEAP.

BET analysis was carried out in order to determine the surface area of $CaCO_3$ microparticles and pore size distribution. Nitrogen adsorption−desorption measurements showed a surface area of 8.8 ± 0.3 m^2/g. Taking into account the average weight of one microparticle, the surface area of a microparticle is 7.72×10^{-10} m^2. Theoretical calculation of the surface area of nonporous microparticles (microbeads) with the same average size gives us the value 7.11×10^{-11} m^2. Thus, for $CaCO_3$ microparticles used in this study we have a surface area that is 11 times larger due to porous structure. The pore distribution in size is presented in Figure 3B. One can see the size of microparticle pores is mostly from 20 to 60 nm and the average pore size was determined to be 35 nm.

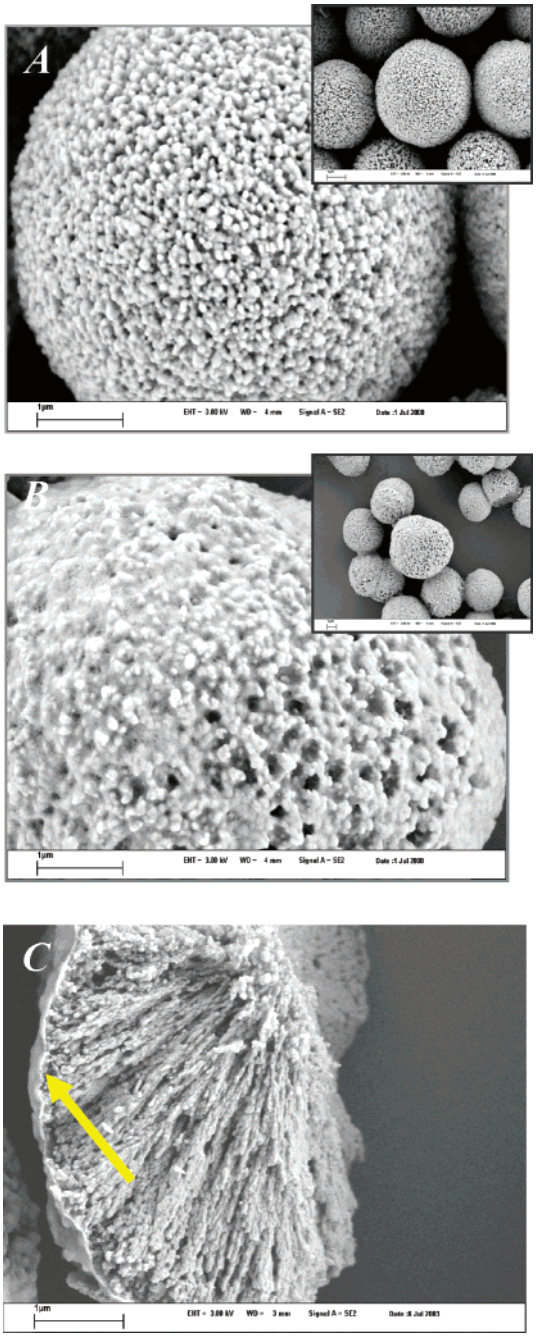

Figure 4. SEM images of $CaCO_3$ microparticles treated by 6 (A) and 16 (B,C) PEAP. Scale bar = 1 μm.

Determination of the surface charge of $CaCO_3$ microparticles in a particle suspension in water was carried out employing electrophoretic mobility measurements. The ξ-potential of microparticles was determined to be −12.2 mV. Because of the negative charge of microparticles, the first polyelectrolyte used for consecutive treatment was PAH which is positively charged. An alternating change of ξ-potential during polyelectrolyte adsorption was observed (Figure 3C). This indicates adsorption of polyelectrolytes on each PEAP.

SEM micrographs of $CaCO_3$ consecutively treated by PSS and PAH solutions (6 and 16 PEAP) are presented in images A and B of Figure 4, respectively. We can see that the surface of the coated particles was found to be rougher compared to the surface of the initial $CaCO_3$ microcores. This can be explained by the formation of a polyelectrolyte net onto the particle surface, which shrinks when dried for SEM measurements. The larger the number of PEAP used, the greater the adsorption of polyelectrolytes, resulting in a pronounced surface coating (Figure 4C). One can clearly see the formation of a polyelectrolyte film on the surface of the broken particle (arrow in Figure 4C). It is obvious that the adsorption onto the surface of microcores is more expressed on account of a greater accessibility for polyelectrolytes when 16 polyelectrolyte adsorption procedures were done. The internal structure remains still porous, but from the SEM picture one cannot conclude exactly on the presence of polyelectrolyte complex in the interior.

After the desirable number of PEAP was achieved, the calcium carbonate support was decomposed. This was accomplished by multiple washings in an EDTA solution that leads to the formation of a water-soluble complex between EDTA and Ca^{2+}. Thus, the microcapsules are formed. No peak corresponding to calcium in the capsules was detected by the energy dispersive X-ray method. This indicates a relatively low content of calcium (<0.1% of the sample by weight) could be present but not resolved by this method. Apparently, the rest of the calcium in formed microcapsules can be attributed to Ca^{2+} in contact with sulfonate groups of PSS but the solid core material was dissolved during treatment with EDTA.

SEM images of capsules obtained using 6 and 16 PEAP are shown in images A and B of Figure 5, respectively. The number of PEAP used affects the morphology of the structures formed. In the case of 6 PEAP, the capsule structure looks like a very porous network with many holes (Figure 5A). The surface morphology of the initial $CaCO_3$ microcores governs the morphology of the polyelectrolyte film formed on its surface and as a consequence the morphology of the capsules. After 16 PEAP, the morphology of the capsules differs from that which was described for 6 PEAP. SEM images of such capsules are given in Figure 5B. These capsules have exact folds indicating a visibly thicker wall, which is smoother than the previous capsules (6 PEAP) but still rough. Formation of polyelectrolyte complex on the surface of $CaCO_3$ cores hinders the diffusion of other polyelectrolytes during further treatment with PSS and PAH; this leads to formation of a thick wall in the case of 16 PEAP.

To determine the presence of a polyelectrolyte complex inside the capsule, scanning confocal Raman spectroscopy and CLSM were used. Raman spectra corresponding to signals from the microcapsule wall and the interior for capsules obtained by 16 PEAP are shown in Figure 6A. Pronounced peaks with experimental frequencies of 1125 and 1600 cm^{-1} are shown, which were assigned to the vibration of the sulfonate groups and the aromatic ring quadrant stretching in the PSS molecule. These were detected both on the wall as well as within the interior of the capsules. Peaks found in the Raman spectra indicate the presence of PSS inside the formed microcapsules. In Figure 6B, the CLSM image of microcapsules (16 PEAP) prepared using PAH−FITC is presented. With fluorescence inside the capsules, it is evident that PAH is also in the capsule interior. Thus, both polyelectrolytes were observed to be inside the microcapsule forming a polyelectrolyte complex, which means microcapsules have a matrix type structure and polyelectrolyte complex is not precipitated at the wall. The polyelectrolyte complex between PSS and PAH inside the capsule may have an excess charge due to nonstoichiometry and therefore swell, remaining within the capsule forming a gel-like structure. The diameter of the pores in the $CaCO_3$ microparticles is from 20 to 60 nm. This allows small molecules of PSS and PAH with a size of several nanometers to penetrate inside

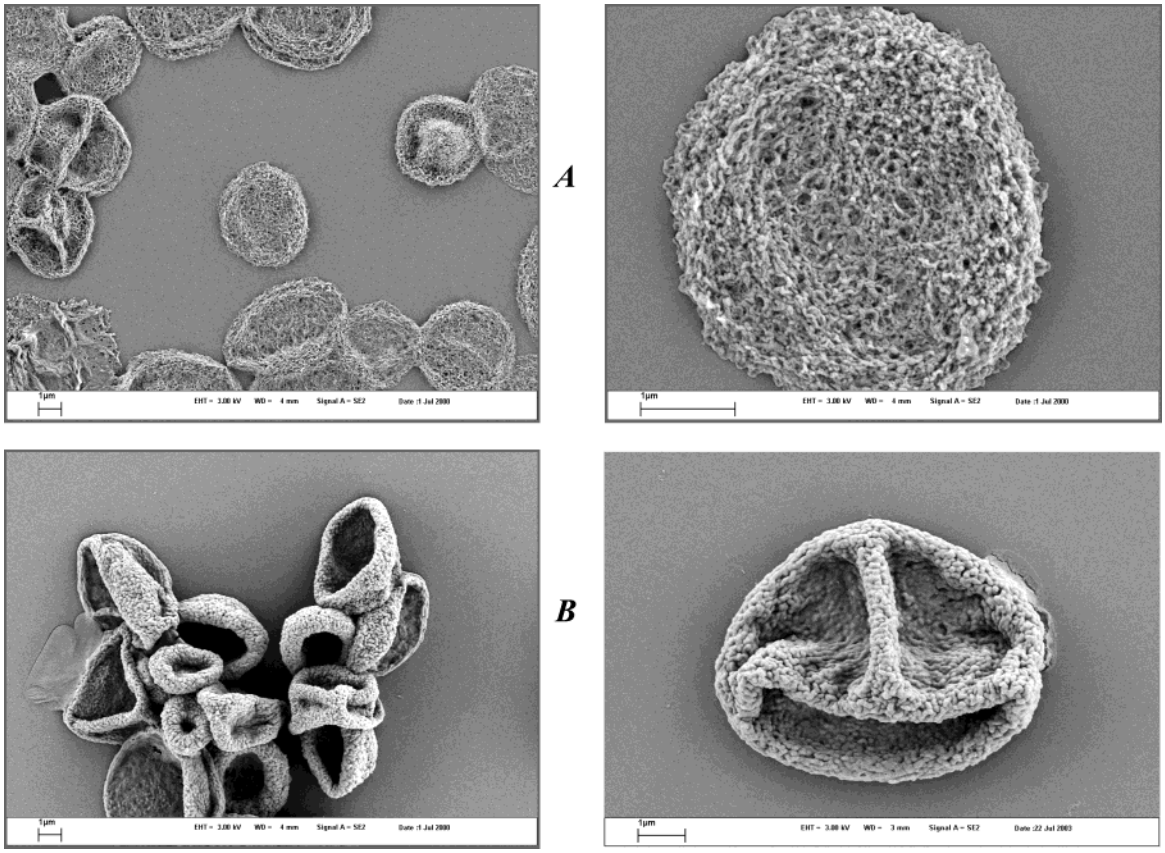

Figure 5. SEM images of microcapsules prepared using 6 (A) and 16 (B) PEAP. Scale bar = 1 μm.

through the pores during consecutive polyelectrolyte treatments forming a polyelectrolyte complex which remains stable after the core dissolution.

SFM images of microcapsules (6 PEAP) in overview (Figure 7A), three-dimensional presentation (Figure 7B), and in the zoomed region (Figure 7C) are presented together with a cross section (Figure 7D). The thickness of a 6 PEAP capsule was found to be 95 nm. The thickness of one polyelectrolyte layer (PSS or PAH) adsorbed onto a smooth charged surface of colloid particle is approximately 1.5 nm.[12] The thickness of one polyelectrolyte layer of films of PSS/PAH was found to be about 1.3 nm using atomic force microscopy (AFM) measurements of dried capsules,[12c] which is in agreement with the value of 1.5 nm for one layer obtained in a solution of capsules by single-particle light scattering.[12a,b] In the case of capsules prepared in this study, the same polyelectrolytes and adsorption conditions were used. For the capsules prepared on $CaCO_3$ microtemplates, the thickness contribution of one adsorption procedure was calculated as 8 nm, which is 5 times greater than that for fabrication on smooth surfaces. To all appearances, a strong increase in thickness can be attributed to the texture of initial $CaCO_3$ microtemplates but not to water remaining in dry capsules. It is assumed that polyelectrolyte adsorption onto the very rough surface of $CaCO_3$ microcores promotes the formation of such a thick and porous polyelectrolyte network of the capsule wall. It is obvious that the polyelectrolyte complex (matrix) inside the capsule also has a considerable share in the thickness increase; this however cannot be estimated.

Such a dense network structure of the capsule wall allows a capsule to be very stable. The increase of osmotic pressure would be expected during core dissolution, which is caused by fast flowing Ca^{2+} and CO_3^{2-} ions from the core interior out to the surrounding solution. This could affect the structure and properties of the polyelectrolyte complex formed by consecutive treatments of PSS and PAH. It is known that when melamine formaldehyde cores were used for capsule formation, the transient high osmotic pressure resulted in significant capsule swelling and even rupturing of the capsule wall.[13] The size distribution of the capsules (6 PEAP) was found to be dependent on the core but not on the dissolution procedure. This can be concluded from the fact that the size distributions of the cores and of the capsules are basically identical (Figure 3). We suppose that the polyelectrolyte complex formed on the surface/inside of the capsule creates a strong but porous net, which protects the capsule from high osmotic pressure allowing Ca^{2+} ions to penetrate rapidly through the pores but not destroying them.

Macromolecule Encapsulation into Microcapsules. Many water-soluble substrates such as dyes, polyelectrolytes, and proteins can accumulate spontaneously inside multilayer polyelectrolyte microcapsules, which were produced on melamine formaldehyde microparticles (MF particles) using the LbL technique with PSS and PAH.[14] Recently, the accumulation of proteins in microcapsules templated on MF particles and their controlled release from capsules were reported.[15] The

(12) (a) Sukhorukov, G. B.; Donath, E.; Davis, S.; Lichtenfeld, H.; Caruso, F.; Popov, V. I.; Möhwald, H. *Polym. Adv. Technol.* **1998**, *9*, 759. (b) Sukhorukov, G. B.; Donath, E.; Lichtenfeld, H.; Knippel, E.; Knippel, M.; Budde, A.; Möhwald, H. *Colloids Surf., A* **1998**, *137*, 253. (c) Leporatti, S.; Voigt, A.; Mitlohner, R.; Sukhorukov, G. B.; Donath, E.; Möhwald, H. *Lanqmuir* **2000**, *16*, 4059.

(13) Gao, C. Y.; Moya, S.; Lichtenfeld, H.; Casoli, A.; Fiedler, H; Donath, E.; Möhwald, H. *Macromol. Mater. Eng.* **2001**, *286*, 355.

(14) Gao, C. Y.; Donath, E.; Möhwald, H.; Shen, J. *Angew. Chem., Int. Ed.* **2002**, *41* (20), 3789.

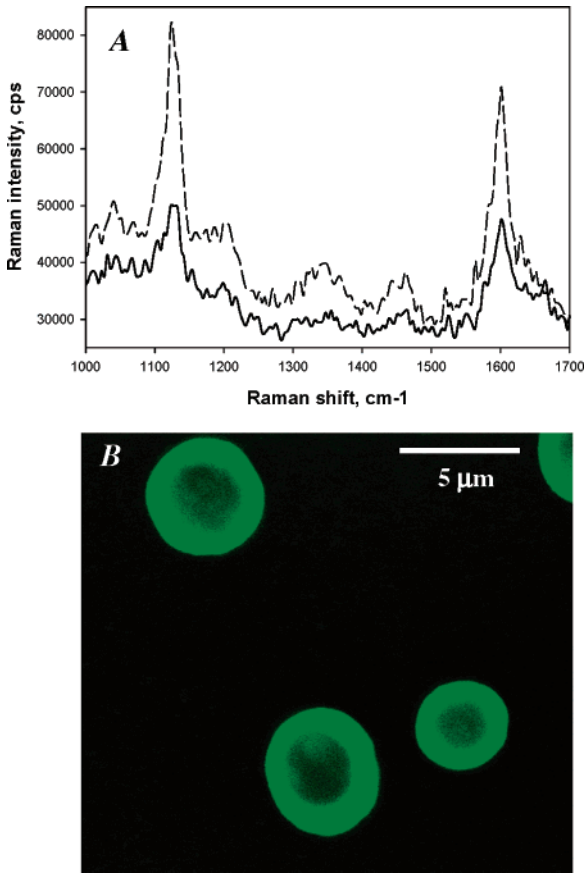

Figure 6. Raman spectra of microcapsules, 16 PEAP (A). The dashed curve corresponds to the signal from the capsule wall, and the solid curve to the signal from the capsule interior. CLSM image of microcapsules (16 PEAP) prepared using PAH−FITC and PSS (B).

formed microcapsules were shown to be of a matrix type capsule and to have a gel-like structure consisting of the remaining melamine formaldehyde resin and polyelectrolytes used for capsule preparation.

Microcapsules formed by this technique were used as supports for macromolecule entrapment. Adding BSA and dextran into the capsule suspension resulted in the capture and spontaneous accumulation of macromolecules from the surrounding medium. Because BSA is negatively charged, PSS was chosen as the first polyelectrolyte to start LbL assembly to reduce protein adsorption on the surface of capsules. Figure 8 shows micrographs of microcapsules (16 PEAP) filled with BSA labeled by FITC after incubation of capsules in a solution of protein and washing with water. The same images were observed for dextran−FITC. BSA−FITC and dextran−FITC were strongly adsorbed in the wall of the microcapsules with 16 PEAP as well as in the interior as the fluorescent profile shows (Figure 8D). The cross section profile of fluorescence gives information about the distribution of labeled dextran in the capsule. The very porous structure of the microcapsules offered no difficulties for macromolecules to permeate into them and to attach to the matrix, forming an interpenetrating polyelectrolyte network. Therefore, the fluorescent profile reflects the density of the polyelectrolyte complex (more polyelectrolytes, more charges, more adsorbed material). According to the profile, polyelectrolyte concentration is decreased toward the center of the microcapsule, which can be explained by diffusion limitations when PSS and PAH permeated through the pores of $CaCO_3$ microparticles. With the next adsorption step of polyelectrolytes, the pore size is decreased due to adsorption of polyelectrolytes. Moreover, polyelectrolyte complex PSS−PAH can be formed not only onto the surface of the internal particle volume but also directly in the pores if polyelectrolyte was not completely removed from the pores during the washing procedure. This makes it difficult to move polyelectrolytes to the center of the microcore.

Dissolution of the $CaCO_3$ microcore led to more or less uniform gel-like matrix formation inside the capsule or to the presence of clusters of polyelectrolyte complex (Figure 8A). The arrow in this figure points at pronounced fluorescence from the part of the internal volume of the microcapsule that is concerned with accumulation of

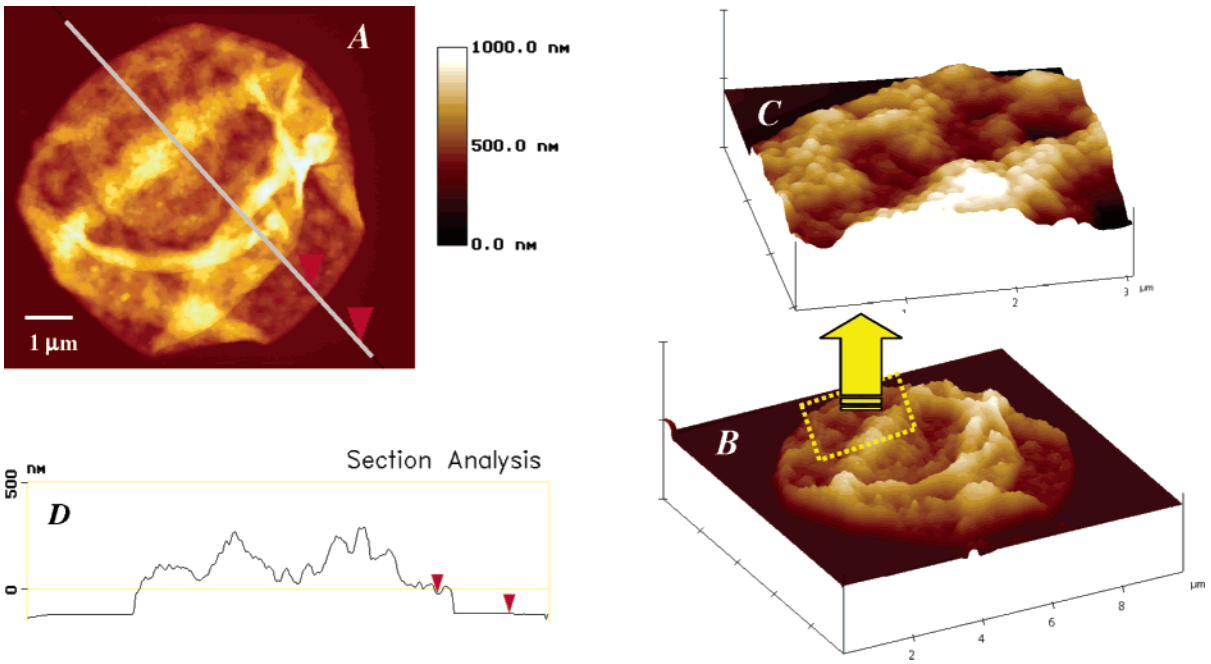

Figure 7. Typical SFM images of a microcapsule (6 PEAP): (A) top view, (B) three- dimensional presentation, (C) high-resolution SFM image of the region of image B, and (D) cross section of the capsule presented in image A.

Table 1. Weights of Microparticles Used in This Study

$CaCO_3$ microparticle, pg (QCM)	number of PEAP	fabricated microcapsule, pg (QCM)	amount of dextran−FITC/BSA−FITC adsorbed per capsule, pg	
			fluorescence spectroscopy	QCM
88.6 ± 7.6	6	10.6 ± 0.6	5.6 ± 0.3/12.0 ± 0.9	6.1 ± 0.5/10.4 ± 1.3
	16	23.8 ± 1.4	8.9 ± 0.5/14.5 ± 0.7	9.3 ± 0.5/15.0 ± 1.1

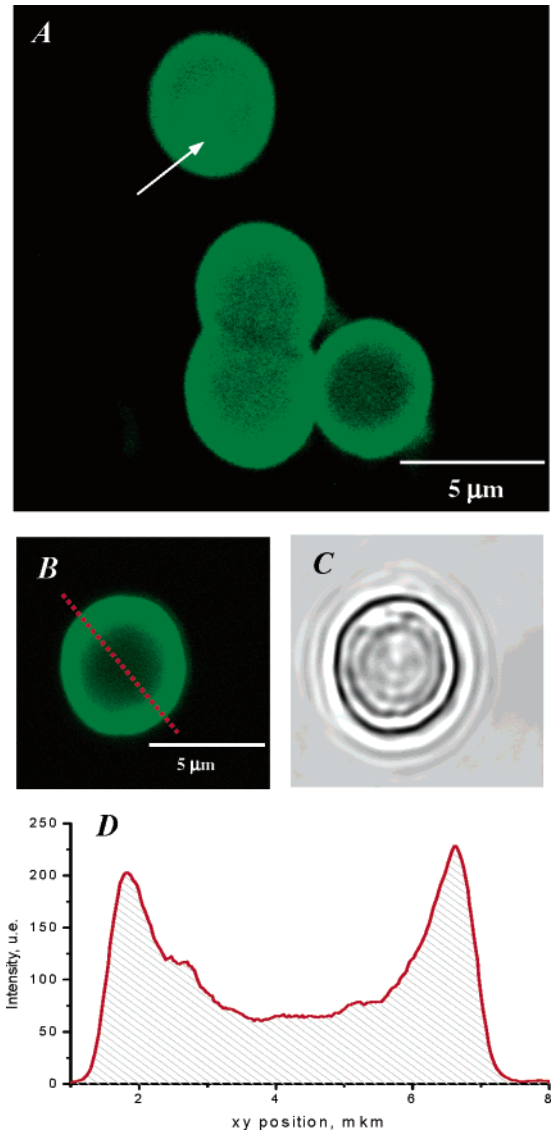

Figure 8. CLSM images of microcapsules (16 PEAP) after incubation with BSA−FITC (A) and dextran−FITC (B) followed by water washing. (C) Transmission confocal microscopy image of the capsule presented in image B. (D) The fluorescence profile for image B.

polyelectrolyte complex in this region. The presence of the clusters can be caused by uneven formation of complex PSS−PAH in the pores of $CaCO_3$ particles during consecutive polyelectrolyte treatment.

Accumulation of BSA and dextran inside microcapsules was observed for 3-month-old capsules stored in water, which means the matrix of polyelectrolyte complex is stable and remains inside the capsule for a long time.

Table 1 presents data of weights of native microcores, polyelectrolyte-treated cores, formed capsules, and also the amount of BSA or dextran entrapped in microcapsules with different numbers of PEAP. The average weight of a single $CaCO_3$ microcore was calculated to be approximately 88 pg, whereas capsules fabricated were found to be only 11 and 24 pg for 6 and 16 PEAP, respectively. It is obvious that this large decrease in weight is caused by the loss of solid carbonate core support. The weight of polyelectrolyte microcapsules is very high. The weight of one hollow microcapsule from PSS and PAH (8 PEAP) prepared onto a smooth colloid surface was found to be about 1.4 pg.[5a] Such high mass of the capsule prepared in this study is attributed to the presence of a polyelectrolyte complex inside the capsule and larger adsorption of polyelectrolytes on the very rough surface of $CaCO_3$ microsupports. The increase in the PEAP number from 6 to 16 leads to a weight increase of more than twice because of the extended polyelectrolyte treatments.

Fluorescence spectroscopy and QCM analysis were used to determine the amount of BSA/dextran adsorbed in microcapsules. The results were found to be analogous for the two independent analyses. For this task, we compared the fluorescence signal from microcapsules filled with dextran−FITC and BSA−FITC to signals from clear dextran−FITC and BSA−FITC solutions with a wide range of concentrations due to the nonlinear dependence between the signal and the concentration of a fluorescent compound. It is important that microcapsules at the used concentration did not influence the fluorescence of dextran−FITC and BSA−FITC solutions in this experiment and did not give a high background.

The amount of dextran adsorbed was 6 and 9 pg for a capsule with 6 and 16 PEAP, while for BSA it was found to be 12 and 16 pg, respectively. One can see that with an increase in the number of PEAP from 6 to 16, the amount of macromolecules adsorbed increased by 50%. For all experiments, the quantity of BSA adsorbed was determined to be 80−90% greater than for dextran. Obviously this can be explained by electrostatic interaction between free amino and sulfonate groups of polyelectrolyte complex inside the microcapsule and surface charges of amino acids of protein BSA, whereas the dextran molecule is not charged. Apparently, electrostatics has considerable contribution to the interaction between microcapsules and macromolecules.

Microcapsules have a very high capacity for BSA and dextran entrapment. Thus one capsule (6 PEAP) can adsorb more than 10 pg of BSA, which is equal to its own weight. For a capsule with 16 PEAP, the weight was 24 pg and the amount of BSA adsorbed was found to be 15 pg. This is not equal to the capsule weight and can be attributed to the reduced number of free charged groups in the denser wall of the capsule with increased number of PEAP. Taking into account that 15 pg of BSA was adsorbed into a microcapsule with an average size of 4.5−5.0 μm, the average concentration of protein per one capsule can be calculated to be more than 250 mg mL^{-1}, indicating that the adsorbed material is in complexed or aggregated form rather than in a free state.

Conclusion

In summary, we demonstrated a novel approach to fabricate polyelectrolyte microcapsules with a gel-like matrix of polyelectrolytes inside. The process of consecutive polyelectrolyte adsorption applied to porous calcium carbonate microparticles as templates results in poly-

(15) Balabushevich, N. G.; Tiourina, O. P.; Volodkin, D. V.; Larionova, N. I.; Sukhorukov, G. B. *Biomacromolecules* **2003**, *4* (5), 1191.

electrolyte matrix formation within the templating particles due to permeation of polyelectrolytes into porous microsupports during the LbL assembling procedure. After core decomposition, the formed microcapsules have a matrix type structure consisting of a porous polyelectrolyte network inside. We demonstrated that the encapsulation of macromolecules, such as proteins and polysaccharides, can be performed by adsorption into this matrix within the polyelectrolyte capsules. One capsule can adsorb more than 10 pg of BSA and about 10 pg of dextran, increasing the macromolecule concentration to several hundreds of mg mL^{-1} per capsule. Microcapsule morphology, structure, and adhesion capacity for entrapping macromolecules are influenced by a number of polyelectrolyte adsorption procedures used for capsule preparation. Encapsulation of macromolecules is based presumably on electrostatic interaction between macromolecules and free charges of the polyelectrolyte complex inside the capsules. Thus this type of encapsulation by means of colloidal templating of gel-like matrixes could be used for biological materials with high payload without losing their bioactivity.

Acknowledgment. The work was supported by the Sofja Kovalevskaja Program of the Alexander von Humboldt Foundation and the German Ministry of Education and Research. D. V. Volodkin thanks DAAD for support (Referat 325, Number A/03/01495). The authors are grateful to Prof. Dr. H. Möhwald for reading the manuscript and stimulating discussions. We thank also Wenfei Dong for help with Raman spectroscopy, D. Shchukin for SEM measurements, and Dr. D. Shenoy for reading the manuscript and corrections.

LA036177Z